frontiers in Materials

ORIGINAL RESEARCH
published: 23 August 2021
doi: 10.3389/fmats.2021.727273

Experimental Research on Compressive and Shrinkage Properties of ECC Containing Ceramic Wastes Under Different Curing Conditions

Yan Xiong[1,2]*, Yi Yang*[1]*, Shuai Fang*[1]**, Di Wu*[3] *and Yingfeng Tang*[4]

[1]*School of Civil Engineering and Transportation, South China University of Technology, Guangzhou, China,* [2]*State Key Laboratory of Subtropical Building Science, South China University of Technology, Guangzhou, China,* [3]*Earthquake Engineering Research and Test Center, Guangzhou University, Guangzhou, China,* [4]*Guangzhou Pearl River Foreign Investment Architectural Design Institute Co. Ltd, Guangzhou, China*

Engineered cementitious composites (ECCs) suffer from high shrinkage and low early strength due to large dosage of cementitious materials and slow hydration of fly ash. This study aims to improve compressive properties and reduce drying shrinkage of ECC using ceramic wastes and hydrothermal curing. Experimental results have indicated that ceramic polishing powder (CPP) and recycled ceramic sand (RCS) exert opposite effect on the compressive strength of ECC. Hydrothermal-cured ECC enhances elasticity modulus and compressive strength and reduces later drying shrinkage as compared with that under standard curing. A CPP dosage of 35% and a hydrothermal curing regime with a temperature of 70°C and age of 7 days are recommended for the engineering application of ECC.

Keywords: ECC, compressive property, shrinkage, ceramic waste, curing condition

OPEN ACCESS

Edited by:
Kequan Yu,
Tongji University, China

Reviewed by:
Li Yazhao,
Nanyang Technological University, Singapore
Dan Meng,
Nanyang Technological University, Singapore

****Correspondence:***
Shuai Fang
fangshuai@scut.edu.cn

Specialty section:
This article was submitted to Structural Materials, a section of the journal Frontiers in Materials

Received: *18 June 2021*
Accepted: *28 July 2021*
Published: *23 August 2021*

Citation:
Xiong Y, Yang Y, Fang S, Wu D and Tang Y (2021) Experimental Research on Compressive and Shrinkage Properties of ECC Containing Ceramic Wastes Under Different Curing Conditions.
Front. Mater. 8:727273.
doi: 10.3389/fmats.2021.727273

INTRODUCTION

Compared with common cement-based materials, the engineered cementitious composite (ECC) has excellent ductility, impact strength, and fracture resistance (Li, 2003). It exhibits strain-hardening and multiple cracking behaviors with ultimate strain exceeding 3% under uniaxial tension (Li et al., 2001). Because of these significant advantages, ECC has become increasingly popular in the field of civil engineering. However, ECC produces large drying shrinkage due to the high content of cementitious materials. Its 28-day shrinkage strain can reach up to 1,200–1,800 με (Gao et al., 2018). Such large shrinkage causes high tensile stress and even cracks in ECC, which degrades the stiffness and resistance to penetration. When ECC is utilized as the repairing and connecting material, the shrinkage weakens the bond between the ECC and the substrate (Li and Li, 2006). The high dosage of fly ash in ECC even causes low early strength, which leads to long curing time and slow turnover of formwork. In addition, the cementitious materials and quartz sand increase the cost of ECC. The above-mentioned shortcomings hinder the application of ECC in engineering.

High-temperature curing, including steam curing and hydrothermal curing, can effectively activate pozzolanic reaction and elevate the early hydration degree of cementitious materials. More hydration products generate on the surface of cementitious particles, which makes the microstructure denser (Hanehara et al., 2001). As a result, the early strength of cement-based materials is significantly improved. The high-temperature curing also shortens the curing time and production cycle, speeds up the turnover of the mold, and improves the production efficiency (Wu et al., 2017; Liu et al., 2020). Studies have demonstrated that steam curing improves the bond performance of the fiber-cement matrix interface. The strength and fracture energy of the interface show an upward trend with increasing curing age (Zhu et al., 2011; Wei, 2017). Besides the mechanical properties, the shrinkage of concrete can be reduced by high-temperature curing (Richard and Cheyrezy, 1995).

Ceramic polishing powder (CPP) is a by-product from grinding and polishing processes of ceramic tile production. Benefited by the small particle size and glass phase, CPP has high pozzolanic activity, which makes it an ideal substitute to replace cement or fly ash (Ay and Ünal, 2000; Wang et al., 2011). Wang et al. (2012) found that CPP as an admixture can exert secondary hydration effect, refine the pore structure of the hardened cement paste, and inhibit the alkali-aggregate reaction. Li et al. (2019a) indicated that addition of CPP by 20 vol% can reduce the cement content by 33% and increase 7-day and 28-day compressive strength by 85% at least. In addition, CPP can effectively improve chloride resistance of the mortar (Li et al. 2020), substantially decrease autogenous shrinkage of cement paste (Li et al. 2019b), and improve the frost resistance of the mortar (Cao et al., 2014).

In addition as a substitute for cement, qualified hardness and good wear resistance enable ceramic wastes to act as aggregates. Using recycled ceramic sand (RCS) as a replacement to partial sand can lead to various enhancements in the compressive strength, abrasion resistance, workability, resistance to chloride-ion corrosion of concrete, and reduction in the shrinkage of the mortar (Binici, 2007; López et al., 2007; Liu et al., 2015; Nie et al., 2015). However, it was also found that RCS slightly deteriorated workability and compressive strength of masonry mortar and recycled concrete in other studies. This was attributed to high water absorption, slightly low density, and rough surface of the RCS than river sand (Wu et al., 2008). The influence of RCS on mechanical properties of cementitious composites needs to be studied further.

The annual emission of ceramic wastes in China has exceeded 18 million tons. The wastes from Foshan account for one fifth of the national emission (Cai et al., 2011; Wang et al., 2019). However, most of the ceramic wastes are disposed by means of stacking in the open, without any treatment or utilization. The waste particles and dust pollute air, groundwater, and soil, which arouses public concern (Xu et al., 2013). Application of ceramic wastes in ECC is an appropriate method to deal with the wastes from the perspective of economics and environment.

As mentioned above, high-temperature curing can increase early strength and reduce drying shrinkage of cementitious materials. CPP and RCS have great potential to be mineral admixtures and aggregates, respectively. The application of ceramic wastes in ECC will produce additional economic and environmental benefits. This study, therefore, was intended to improve the compressive and shrinkage performance of ECC using ceramic wastes and hydrothermal curing. To this aim, ECC specimens containing ceramic wastes were first cured under various conditions and then subjected to compressive and drying shrinkage tests. The effects of curing conditions and ceramic waste dosages were investigated.

EXPERIMENTAL PROGRAM

Materials and Mix Proportions

The materials used in the production of the ECC mixture consisted of cementitious materials, aggregates, fibers, and additives.

Cementitious Materials

Class 42.5R ordinary Portland cement and Class F fly ash were used as the binders of the control mixture. The fly ash had a specific surface area of 362 m^2/kg. CPP was utilized as an alternative to fly ash. The chemical composition of cement, fly ash, and CPP is presented in **Table 1**. Similar to fly ash, CPP was mainly composed of aluminosilicate. The residue on the 45 μm sieve of cement, fly ash, and CPP was 10.2, 11.2, and 3.1%, respectively, which meets the requirement as cementitious materials. The particle sizes of the cementitious materials are illustrated in **Figure 1**. CPP had fineness between that of cement and fly ash.

Aggregates

Quartz sand and RCS with the size of about 100 mesh were used as the aggregates of ECC. As illustrated in **Figure 2**, RCS was obtained by crushing and milling ceramic tile fragments and configuration according to the gradation of quartz sand. The microtopography of both aggregates was taken using a scanning electron microscope. Both RCS and quartz sand had sharp edges and rough surfaces, while there were more large particles and chippings in the former (**Figure 3**). This is also verified by the size distribution of aggregates in **Figure 1**. RCS particles had close median size while wider distribution than quartz sand.

Fibers

The fibers used were polyvinyl alcohol (PVA) fibers and basalt fibers (**Figure 4**). Detailed properties of the fibers are summarized in **Table 2**.

Additives

A superplasticizer with a water reducing rate of 20% and a hydroxypropyl methyl cellulose-based thickener were used to improve the workability of ECC in this study.

Mix Proportions

As shown in **Table 3**, a total of three mixture proportions were adopted. P0 was the control mixture without any ceramic waste. P1 replaced half of fly ash by CPP. P1S1 further replaced half of quartz sand by RCS based on P1. The constant water-binder ratio of 0.35, the PVA fiber dosage of 1.5vol%, and the basalt fiber dosage of 0.5vol% were kept for all mixtures (Tang, 2020).

TABLE 1 | Chemical composition of the cementitious materials (%).

Materials	SiO_2	Al_2O_3	Fe_2O_3	CaO	MgO	SO_3	K_2O	Na_2O	Cl^-	Loss on ignition
Cement	19.57	7.69	2.39	59.21	2.84	2.45	0.59	—	0.06	3.20
Fly ash	53.97	31.15	4.16	4.01	1.01	0.73	2.04	—	0.13	2.67
CPP	69.04	16.92	0.77	1.43	1.38	—	2.17	2.17	0.58	2.93

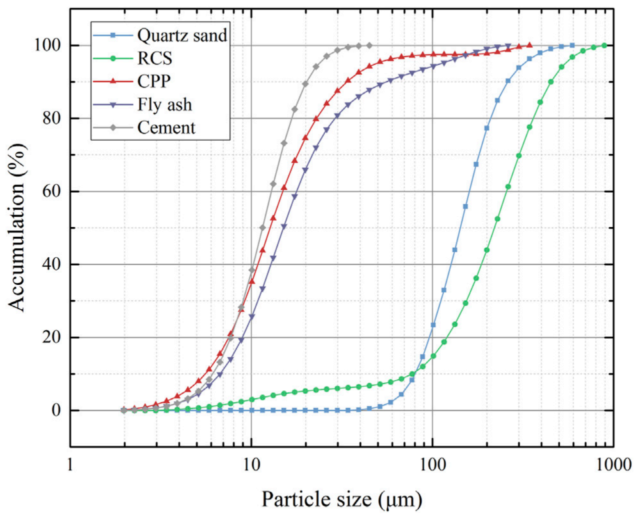

FIGURE 1 | Size distribution of cementitious materials and aggregates.

Preparation of Specimens

Cementitious materials, aggregates, and thickener were first mixed for about 3–4 min. Water and superplasticizer were then added and mixed for the next 2–3 min until the mixture was homogeneous. Basalt fibers and PVA fibers were added with an interval of 1 minute to avoid clustering. The mixture was then mixed at high speed for three additional minutes.

The fresh mixture was cast into molds and compacted on a vibrating table. The specimens were subsequently placed indoors for 24 h with a polyethylene film on them.

Curing Conditions

After reaching the age of 24 h, the specimens were removed from the moulds and subjected to various curing schemes. Five curing schemes, including standard curing and four hydrothermal ones, were adopted (**Table 4**). The temperature and relative humidity for the standard curing were set according to the Chinese standard GB/T 17671-1999 (SBQTS, 1999). For the hydrothermal curing, the specimens were immersed in a hot water controller equipped with a thermostat. The upper temperature of hydrothermal curing was set at 70°C, according to the Chinese standards GB/T 31387-2015 (AQSIQ and SAC, 2015) and JG/T 565–2018 (MHURD, 2018). Hydrothermal cured specimens were cooled down to room temperature before compression and shrinkage tests.

Axial Compression Tests

Axial compression tests were carried on ECC specimens with reference to the Chinese standards CECS 13-2009 CECS (2009) and JGJ/T 70-2009 (MHURD, 2009). In consideration of the loading capacity of the testing machine, cylindrical specimens

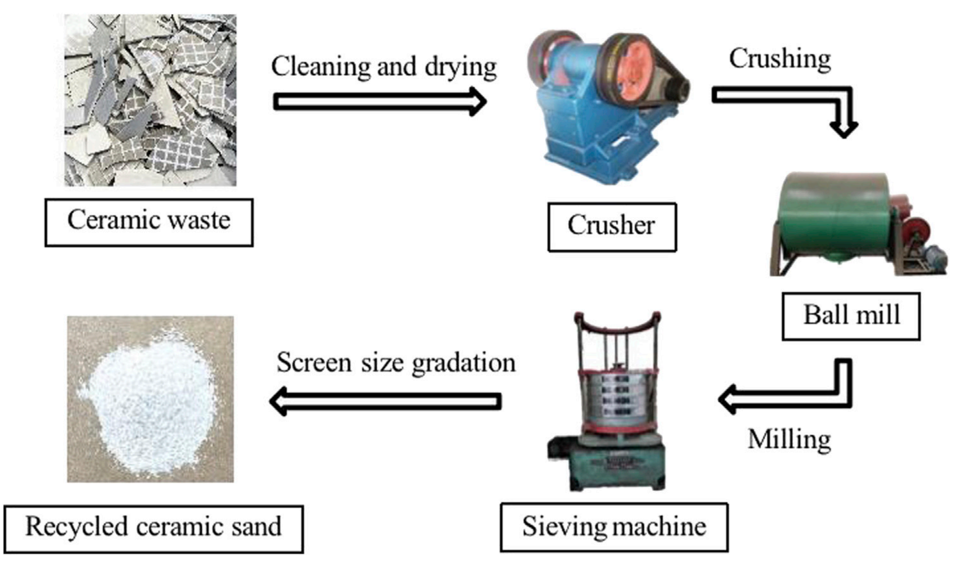

FIGURE 2 | Preparation of RCS.

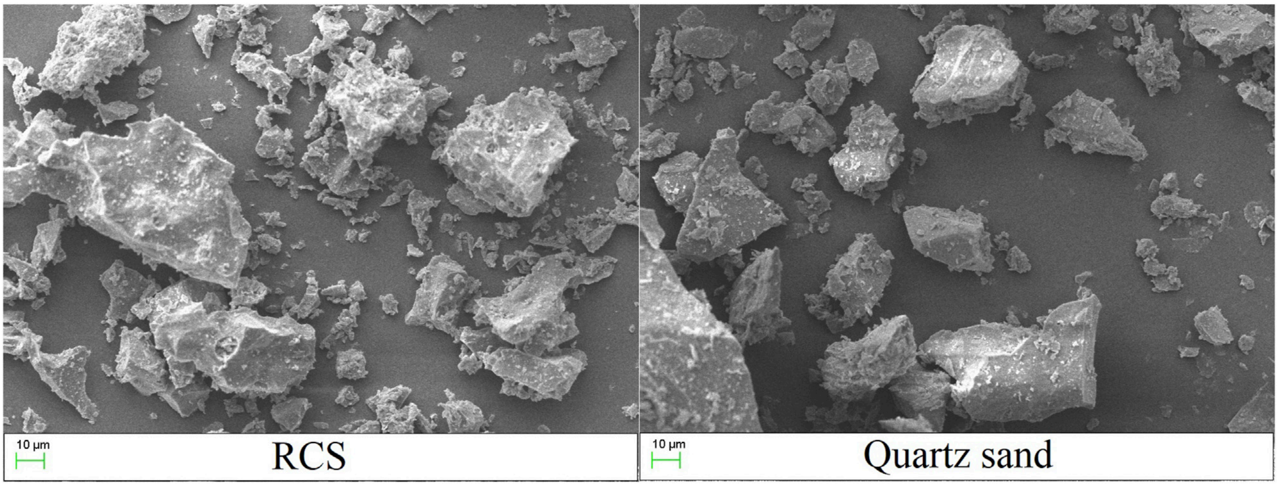

FIGURE 3 | Scanning electron microscope images of RCS and quartz sand.

FIGURE 4 | Images of PVA fibers and basalt fibers.

TABLE 2 | Material properties of fibers.

Fiber	Density (g/cm^3)	Diameter (μm)	Length (mm)	Tensile strength (MPa)	Elastic modulus (GPa)	Elongation (%)
PVA fiber	1.30	40	12	1,560	41	6.50
Basalt fiber	2.65	17	9	2,750	90.1	2.92

TABLE 3 | Mix proportions of ECC (kg/m^3).

Mixture ID	Cement	Fly ash	CPP	Quartz sand	RCS	Water	Superplasticizer	Thickener
P0	323.2	754.2	0	355.5	0	377.1	1.26	0.54
P1	323.2	377.1	377.1	355.5	0	377.1	1.91	0.54
P1S1	323.2	377.1	377.1	177.8	177.8	377.1	1.91	0.54

TABLE 4 | Description of curing schemes.

Test ID	Curing method	Temperature (°C)	Time
H2D0	Standard curing	20	7 days for shrinkage test and 28 days for compressive test
H5D3	Hydrothermal curing	50	3 days
H5D7	Hydrothermal curing	50	7 days
H7D3	Hydrothermal curing	70	3 days
H7D7	Hydrothermal curing	70	7 days

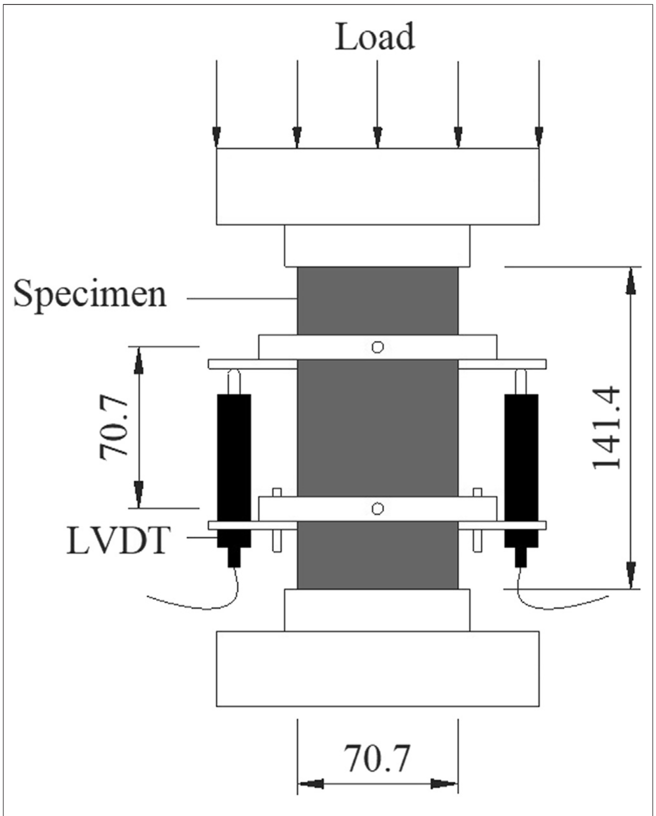

FIGURE 5 | Schematic view of the compression test (unit: mm).

FIGURE 6 | Failure mode of specimens after the compression test.

with a height of 141.4 mm and a diameter of 70.7 mm were employed. Three specimens were prepared for each mix proportion under each curing scheme. Before the test, gypsum was used to cap both ends of the specimens to level. As shown in **Figure 5**, a pair of LVDTs was installed in the middle of the specimens with a gauge length of 70.7 mm to measure axial deformation. Axial load with a rate of 0.5 mm/min was applied using an electrohydraulic servo tester. The loads and axial deformation were recorded synchronously with a data acquisition instrument. The elastic modulus of ECC specimens was calculated based on the specification in the Chinese standard JGJ/T 70-2009 (MHURD, 2009).

Shrinkage Tests

Drying shrinkage of ECC after curing was tested in accordance with JGJ/T 70–2009 (MHURD, 2009). Prismatic specimens for the shrinkage test had dimensions of 40 mm × 40 mm × 160 mm. After curing, the initial length of specimens was recorded. The specimens were then placed in an environmental chamber under a temperature of 20°C and a relative humidity of 60%. The shrinkage values were recorded on the 7th, 14th, 21st, and 28th day of the test.

RESULTS AND DISCUSSION

Compressive Properties

Figure 6 shows the failure mode of specimens after axial compression. It was evident that the cracks were mostly diagonal. The existence of fibers prevented specimens from peeling off. This is linked to the bridging effect of fibers which limits the development of cracks and improves the ductility of ECC (Lin et al., 2019). The incorporation of ceramic waste and the hydrothermal curing resulted in little change on the failure mode of ECC.

The stress–strain relationships of specimens under axial compression are plotted in **Figure 7**. As compared with standard cured specimens, hydrothermal cured ones exhibited much higher stiffness and peak stress, but slightly less peak strain.

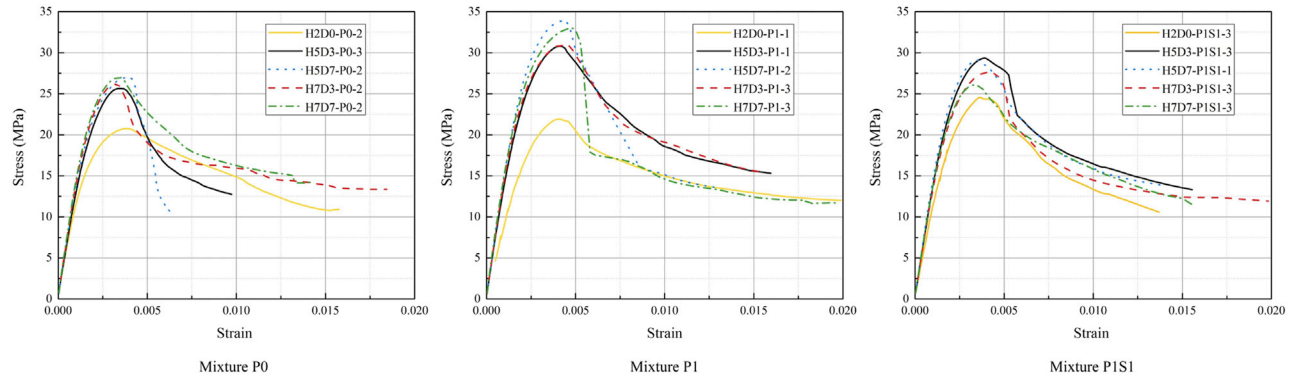

FIGURE 7 | Stress–strain relationships of ECC specimens under compression.

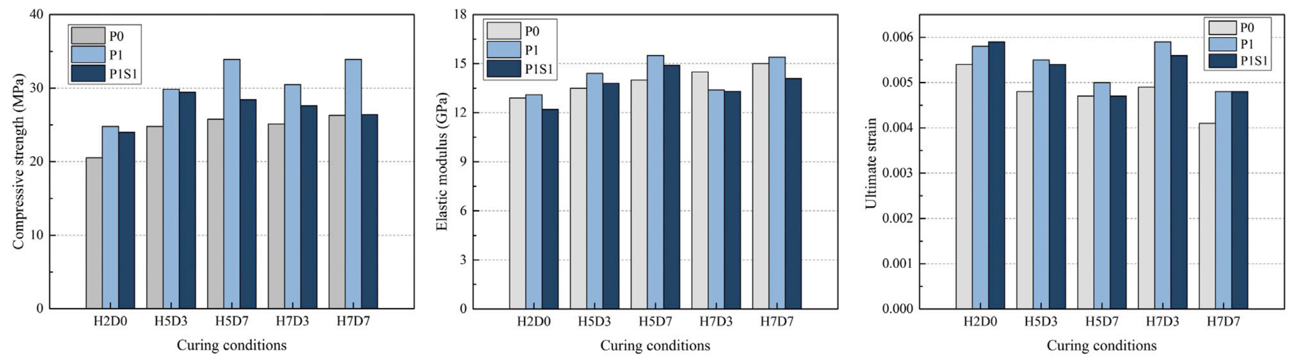

FIGURE 8 | Compressive strength, elastic modulus, and peak strain of ECC.

Mixture P1 showed the highest compressive strength, followed by P1S1, while P0 ranked last.

The effect of ceramic wastes and curing conditions on the compressive properties of ECC is illustrated in **Figure 8**. Under the standard curing, the replacement of fly ash by CPP increased the compressive strength of P1 specimens by 21%, which is benefited by the finer particles and higher pozzolanic activity of CPP. Previous studies have indicated that CPP can effectively reduce the porosity of matrix, thereby increasing the compressive strength (Tang, 2020; Li et al., 2021; Xiong et al., 2021). CPP also slightly improved the ultimate strain of ECC. This can be explained by the findings of Kulovaná et al. (2016) that a proper amount of CPP was able to enhance the effective fracture toughness of concrete. High fracture toughness raised the threshold for propagation of cracks and thus increased the peak strain of CPP-incorporated ECC.

The replacement of quartz sand by RCS, however, slightly reduced the compressive strength and elastic modulus of the P1S1 specimens, as compared to P1 ones. This phenomenon is mainly ascribed to increasing porosity caused by deteriorative workability of fresh RCS-incorporated mixture. RCS is characterized by higher water absorption than natural aggregate. This reduces actual water for mixing while increases the viscosity of the fresh mixture. The viscous mixture is difficult to be compacted and results in porous microstructures after hardening. The previous mercury intrusion porosimetry results indicated that complete replacement of quartz sand by RCS increased total porosity of matrix by 9.3% (Tang, 2020). In addition, ceramic tiles have Moh's hardness between 4 and 5, which is lower than that of 7 in quartz (Chen, 2017). The inferior hardness affects the performance of RCS under compression.

After hydrothermal curing, ECC specimens elevated both compressive strength and elastic modulus while decreased peak strain. The ranking of the three formulas was approximately the same as that under standard curing, but the gap widened among them. Hydrothermal curing accelerated hydration of the cementitious materials, which magnified the differences in compressive properties (Fathy and Sun, 2014; Gonzalez-Corominas et al., 2016; Huang et al., 2016). Increasing curing temperature to 50°C significantly improved compressive performance of P0 and P1 specimens. When it further increased to 70°C, scarcely any effect was observed. Extension of hydrothermal curing increased elastic modulus while reduced strain capacity of ECC. The long hydrothermal curing also exhibited positive influence in the compressive strength of P0 and P1 specimens, except P1S1 ones. The compressive strength of P1S1 under curing schemes H5D7 and H7D7 was 28.44 and 26.40 MPa, a little lower than that

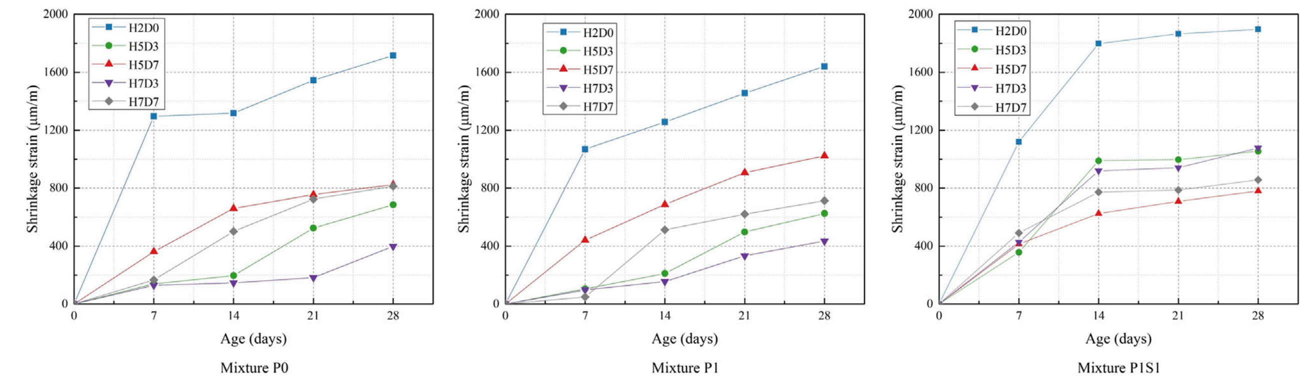

FIGURE 9 | Drying shrinkage of ECC.

of 29.44 and 27.60 MPa under curing schemes H5D3 and H7D3, respectively. The slight deterioration in compressive strength is ascribed to the negative effect of hydrothermal curing on the soundness of RCS. It was found that immersion of RCS in hot water with 70°C for 3 days increased the crushing index of RCS by 14.6% in the preliminary test. The hydrothermal curing schemes of H5D7 and H7D7 are recommended for CPP-incorporated mixture with the consideration of compressive performance of ECC.

Shrinkage Properties

Variation of shrinkage strain with ages is illustrated in **Figure 9**. After the curing, shrinkage grew fast in the first 7 days while slowed down after 14 days. Experimental results showed that replacement of fly ash by CPP had little effect on the shrinkage of ECC, while the incorporation of RCS increased the shrinkage of ECC. This is attributed to the difference in hydration rates between CPP and the fine particles in RCS. The particle size less than 45 μm provided CPP with excellent hydration activity. Most of the shrinkage was achieved in CPP-incorporated specimens during the curing period. However, the fine particles in the RCS were much larger than CPP. This part of fine RCS particles had an activity index of 69, which was lower than that of 91 in CPP (Tang, 2020). This demonstrates a medium hydration activity of the fine RCS particles, which resulted in slow hydration and continuous shrinkage after curing.

Hydrothermal curing can effectively reduce later drying shrinkage of all three mixtures. Compared with the standard curing, hydrothermal schemes H5D3, H5D7, H7D3, and H7D7 reduced 28-day shrinkage of mixture P0 by 60, 52, 77, and 53% while reduced that of mixture P1 by 62, 38, 74, and 57%, respectively. The later shrinkage of P0 and P1 decreased as the curing temperature increased. Higher temperature can promote hydration and strengthen microstructure, which reduces the later shrinkage strain of ECC (Richard and Cheyrezy, 1995). P0 and P1 specimens increased their shrinkage with increasing curing time. Extension of curing promoted hydration of cementitious materials. As one of the hydration products, more adsorbed water grew in the capillaries of the hardened matrix. When the specimens are exposed to dry environment, the adsorbed water evaporated, resulting in shrunk matrix induced by capillary stress (Huang, 2006). However, the shrinkage strain of P1S1 was found to decrease with increasing curing time, opposite to that of P0 and P1. The reason seemed to be linked to the internal curing of RCS. The low apparent density and high water absorption enabled RCS outstanding ability to store water. Long curing time benefited the water storage of RCS and continuous release of water to the surrounding matrix, which relieved the drying shrinkage (Liu and Liu, 2012).

CONCLUSION

In this study, the effect of ceramic wastes and curing conditions on compressive and shrinkage properties of ECC was researched. After standard and hydrothermal curing, ECC specimens were subjected to the axial compression test and dry shrinkage test, respectively. Based on the experimental results, the following conclusions are drawn.

CPP was qualified for effective alternative to fly ash in ECC. Replacement of half fly ash by CPP increased the compressive strength by 20% at least and exerted positive influence in the elastic modulus and peak strain of ECC. CPP had little impact on the drying shrinkage of ECC.

RCS degraded the compressive performance and increases later drying shrinkage of ECC. The preparation technique should be improved to smooth RCS particles.

Hydrothermal curing effectively improved strength development and later volume stability of ECC. CPP-incorporated ECC can increase compressive strength by 37% while decrease 28-day drying shrinkage by 38% at least. Elevating curing temperatures was beneficial to the later volume stability. Extension of curing contributed to the compressive performance of ECC.

It is recommended to cure CPP-incorporated ECC under a hydrothermal environment with a temperature of 70°C for 7 days.

DATA AVAILABILITY STATEMENT

The raw data supporting the conclusions of this article will be made available by the authors, without undue reservation.

AUTHOR CONTRIBUTIONS

YX: methodology, data interpretation, funding acquisition, project administration, resources, supervision, validation, and writing—review and editing. YY: data curation, investigation, visualization, and writing—original draft. SF: conceptualization, data interpretation, formal analysis, investigation, methodology, visualization, and writing—review and editing. DW: project administration, resources, supervision, and validation. YT: conceptualization, data curation, data interpretation, investigation, validation, and writing—original draft. All authors contributed to the article and approved the submitted version.

FUNDING

This work was supported by the National Natural Science Foundation of China (Project Nos. 51878298 and 51778160), Natural Science Foundation of Guangdong Province of China (Project No. 2021A1515012606), Science and Technology Program of Guangdong Province of China (Project No. 2018B02028003), and State Key Laboratory of Subtropical Building Science International Cooperation Open Project of China (Project No. 2019ZA05).

ACKNOWLEDGMENTS

The technical support from the State Key Laboratory of Subtropical Building Science is gratefully acknowledged.

REFERENCES

AQSIQ and SAC (General Administration of Quality Supervision, Inspection and Quarantine of the People's Republic of China), and SAC (Standardization Administration of the People's Republic of China) (2015). *GB/T 31387-2015: Reactive Powder Concrete*(in Chinese). Beijing: Standards Press of China.

Ay, N., and Ünal, M. (2000). The Use of Waste Ceramic Tile in Cement Production. *Cem. Concr. Res.* 30, 497–499. doi:10.1016/S0008-8846(00)00202-7

Binici, H. (2007). Effect of Crushed Ceramic and Basaltic Pumice as fine Aggregates on Concrete Mortars Properties. *Construct. Build. Mater.* 21, 1191–1197. doi:10.1016/j.conbuildmat.2006.06.002

Cai, X., Xi, X., Shui, A., Wu, T., Chen, J., Jian, R., et al. (2011). Study on Preparation of High-Strength-Lightweight Building Materials with Porcelain Polishing Waste. *B. Chin. Ceram. Soc.* 30, 955–959. (in Chinese). doi:10.16552/j.cnki.issn1001-1625.2011.04.023

Cao, C., Wang, G., Liu, S., He, X., and Nie, Y. (2014). Effect of Ceramic Polishing Powder and Polypropylene Fiber on Properties of Mortar. *B. Chin. Ceram. Soc.* 33, 1354–1359. doi:10.16552/j.cnki.issn1001-1625.2014.06.063 CNKI:SUN:GSYT.0.2014-06-020 (in Chinese).

CECS (China Association for Engineering Construction Standardization) (2009). *CECS 13–2009: Standard Test Methods for Fiber Reinforced Concrete*. (in Chinese). Beijing: China Planning Press.

Chen, X. C. (2017). Discussion on Moh's Hardness Testing Method of Ceramic Tiles. *Foshan Ceram.* 27, 44–47. (in Chinese). doi:10.3969/j.issn.1006-8236.2017.06.013

Fathy, S., and Sun, W. (2014). Influence of Different Curing Regimes on the Microstructure and Macro Performance of UHPFRCC. *J. Southeast. Univ.* 30, 348–352. doi:10.3969/j.issn.1003-7985.2014.03.017

Gao, S., Wang, Z., Wang, W., and Qiu, H. (2018). Effect of Shrinkage-Reducing Admixture and Expansive Agent on Mechanical Properties and Drying Shrinkage of Engineered Cementitious Composite (ECC). *Construct. Build. Mater.* 179, 172–185. doi:10.1016/j.conbuildmat.2018.05.203

Gonzalez-Corominas, A., Etxeberria, M., and Poon, C. S. (2016). Influence of Steam Curing on the Pore Structures and Mechanical Properties of Fly-Ash High Performance Concrete Prepared with Recycled Aggregates. *Cem. Concr. Compos.* 71, 77–84. doi:10.1016/j.cemconcomp.2016.05.010

Hanehara, S., Tomosawa, F., Kobayakawa, M., and Hwang, K. (2001). Effects of Water/powder Ratio, Mixing Ratio of Fly Ash, and Curing Temperature on Pozzolanic Reaction of Fly Ash in Cement Paste. *Cem. Concr. Res.* 31, 31–39. doi:10.1016/S0008-8846(00)00441-5

Huang, D., Wang, G., Lu, S., Li, H., and Zhu, M. (2016). Hydration Activity of Ceramic Polishing Powder at Hydrothermal Conditions. *B. Chin. Ceram. Soc.* 35, 561–567. (in Chinese). doi:10.16552/j.cnki.issn1001-1625.2016.02.046

Huang, Y. (2006). *Study on Correlation of Drying Shrinkage between Cement Mortar and Concrete*. [Master's thesis]. [Nanjing]: Nanjing University of Technology. doi:10.7666/d.d023861

Kulovaná, T., Vejmelková, E., Keppert, M., Rovnaníková, P., Keršner, Z., and Černý, R. (2016). Mechanical, Durability and Hygrothermal Properties of Concrete Produced Using Portland Cement-Ceramic Powder Blends. *Struct. Concrete.* 17, 105–115. doi:10.1002/suco.201500029

Li, M., and Li, V. C. (2006). Behavior of ECC/Concrete Layered Repair System Under Drying Shrinkage Conditions/Das Verhalten Eines Geschichteten Instandsetzungssystems aus ECC und Beton Unter der Einwirkung von Trocknungsschwinden. *J. Restor. Build. Monum.* 12, 143–160. doi:10.1515/rbm-2006-6040

Li, V. C., Wang, S., and Wu, C. (2001). Tensile Strain-Hardening Behavior of Polyvinyl Alcohol Engineered Cementitious Composite (PVA-ECC). *ACI Mater. J.* 98, 483–492. doi:10.1089/apc.2006.20.82910.14359/10851

Li, L. G., Zhuo, Z. Y., Zhu, J., Chen, J. J., and Kwan, A. K. H. (2019a). Reutilizing Ceramic Polishing Waste as Powder Filler in Mortar to Reduce Cement Content by 33% and Increase Strength by 85%. *Powder Technol.* 355, 119–126. doi:10.1016/j.powtec.2019.07.043

Li, L. G., Zhuo, Z. Y., Zhu, J., and Kwan, A. K. H. (2020b). Adding Ceramic Polishing Waste as Paste Substitute to Improve Sulphate and Shrinkage Resistances of Mortar. *Powder Tech.* 362, 149–156. doi:10.1016/j.powtec.2019.11.117

Li, L. G., Zhuo, Z. Y., Kwan, A. K. H., Zhang, T. S., and Lu, D. G. (2020). Cementing Efficiency Factors of Ceramic Polishing Residue in Compressive Strength and Chloride Resistance of Mortar. *Powder Tech.* 367, 163–171. doi:10.1016/j.powtec.2020.03.050

Li, L. G., Ouyang, Y., Zhuo, Z.-Y., and Kwan, A. K. H. (2021). Adding Ceramic Polishing Waste as Filler to Reduce Paste Volume and Improve Carbonation and Water Resistances of Mortar. *Aben* 2, 3. doi:10.1186/s43251-020-00019-2

Li, V. C. (2003). On Engineered Cementitious Composites (ECC). *Act* 1, 215–230. doi:10.3151/jact.1.215

Lin, J.-X., Song, Y., Xie, Z.-H., Guo, Y.-C., Yuan, B., Zeng, J.-J., et al. (2020). Static and Dynamic Mechanical Behavior of Engineered Cementitious Composites with PP and PVA Fibers. *J. Build. Eng.* 29, 101097. doi:10.1016/j.jobe.2019.101097

Liu, F., and Liu, J. (2012). Experimental Study on the Internal Curing Effect of Recycled Ceramic Sand in Mortar. *Concrete* 11, 102–103. (in Chinese). doi:10.3969/j.issn.1002-3550.2012.11.034

Liu, J., Liu, F., and Zhang, C. (2015). Dry Shrinkage of Recycled Ceramic Mixed Sand Mortar. *China Concr. Cem. Prod.* 04, 54–58. (in Chinese). doi:10.19761/j.1000-4637.2015.04.014

Liu, Z., Hu, J., Weng, Z., Wang, Y., and Xie, Y. (2020). Research Progress on the Effect of Steam Curing on the Performance of Cementitious Materials. *Concrete* 04, 9–13. (in Chinese). doi:10.3969/j.issn.1002-3550.2020.04.003

López, V., Llamas, B., Juan, A., Morán, J. M., and Guerra, I. (2007). Eco-efficient Concretes: Impact of the Use of White Ceramic Powder on the Mechanical Properties of Concrete. *Biosyst. Eng.* 96, 559–564. doi:10.1016/j.biosystemseng.2007.01.004

MHURD (Ministry of Housing and Urban-Rural Development of the People's Republic of China) (2009). *JGJ/T 70-2009: Standard for Test Method of Basic Properties of Construction Mortar* (in Chinese). Beijing: China Architecture & Building Press.

MHURD (Ministry of Housing and Urban-Rural Development of the People's Republic of China) (2018). *JG/T 565-2018: Standard for Quality Management of Precast Concrete Member Fabricated in the Plant* (in Chinese). Beijing: Standards Press of China.

Nie, Y., Liu, X., Peng, Y., Li, X., and Yang, X. (2015). Performance Study of Recycled Masonry Mortar Produced with Reclaimed Ceramic Tiles. *J. Hunan Univ. Nat. Sci. Ed.* 30, 67–71. (in Chinese). doi:10.13582/j.cnki.1672-9102.2015.01.011

Richard, P., and Cheyrezy, M. (1995). Composition of Reactive Powder Concretes. *Cem. Concr. Res.* 25, 1501–1511. doi:10.1016/0008-8846(95)00144-2

SBQTS (State Bureau of Quality and Technical Supervision)(1999). *GB/T 17671-1999: Test Method for Fluidity of Cement Mortar* (in Chinese). Beijing: Standards Press of China.

Tang, Y. (2020). Experimental Study on ECC Mechanical Properties of Hybrid Fibers Containing Ceramic Waste under Different Curing Conditions. [Master's thesis]. Guangzhou: Guangzhou University. (in Chinese). doi:10.27040/d.cnki.ggzdu.2020.000502

Wang, G. X., Xu, K. J., Zhu, M. Q., and Tian, B. (2011). Pozzolanic Activity of Ceramic Polishing Powder as Cementitious Material. *Msf* 675-677, 135–138. doi:10.4028/www.scientific.net/MSF.675-677.135

Wang, G., Tan, L., Nie, Y., and Tian, X. (2012). Effect of Ceramic Polishing Powder on the Chloride Permeability of Concrete. *B. Chin. Ceram. Soc.* 31, 1564–1570. (in Chinese). doi:10.16552/j.cnki.issn1001-1625.2012.06.012

Wang, S., Wang, C., Wang, Y., Zhang, X., and Chen, Y. (2019). Production and Reutilization of Ceramic Waste. *J. Ceram.* 40, 710–717. (in Chinese). doi:10.13957/j.cnki.tcxb.2019.06.002

Wei, Y. (2017). Mechanical Properties of PVA Fiber/Cement-Matrix Interface and Their Effects on Tensile Properties of SHCC. [Master's thesis]. Wuhan: Wuhan University of Technology, 809307. CNKI:CDMD:2.1019 (in Chinese) .

Wu, X., Li, Y., and Yang, J. (2008). Masonry Mortar and Concrete Producing with Recycled Ceramic Aggregate Producing. *Concr.* 0, 50–52. (in Chinese). doi:10.3969/j.issn.1002-3550.2008.09.017

Wu, Z., Shi, C., and He, W. (2017). Comparative Study on Flexural Properties of Ultra-high Performance Concrete with Supplementary Cementitious Materials under Different Curing Regimes. *Construct. Build. Mater.* 136, 307–313. doi:10.1016/j.conbuildmat.2017.01.052

Xiong, Y., Xu, G., Wu, D., Fang, S., and Tang, Y. (2021). Investigation of Using the Ceramic Polishing brick Powder in Engineered Cementitious Composites. *J. Build. Eng.* 43, 102489. doi:10.1016/j.jobe.2021.102489

Xu, Z., Wei, J., Li, F., Gao, P., Chen, Y., and Yu, Q. (2013). Utilizing Ceramic Waste for Autoclaved Aerated Concrete. *New Build. Mater.* 40, 48–51. (in Chinese). doi:10.3969/j.issn.1001-702X.2013.01.015

Zhu, Y., Yang, Y., Gao, X., and Deng, H. (2011). Effect of Curing Temperature on the Mechanical Properties of Engineered Cementitious Composites. *J. Shenzhen Univ. (Sci. Eng.).* 28, 72–77. (in Chinese). doi:10.3969/j.issn.1000-2618.2011.01.011

Conflict of Interest: YT is employed by Guangzhou Pearl River Foreign Investment Architectural Design Institute Co. Ltd.

The remaining authors declare that the research was conducted in the absence of any commercial or financial relationships that could be construed as a potential conflict of interest.

Publisher's Note: All claims expressed in this article are solely those of the authors and do not necessarily represent those of their affiliated organizations, or those of the publisher, the editors and the reviewers. Any product that may be evaluated in this article, or claim that may be made by its manufacturer, is not guaranteed or endorsed by the publisher.

Copyright © 2021 Xiong, Yang, Fang, Wu and Tang. This is an open-access article distributed under the terms of the Creative Commons Attribution License (CC BY). The use, distribution or reproduction in other forums is permitted, provided the original author(s) and the copyright owner(s) are credited and that the original publication in this journal is cited, in accordance with accepted academic practice. No use, distribution or reproduction is permitted which does not comply with these terms.